JOURNAL OF PROPULSION AND POWER
Vol. 22, No. 3, May–June 2006

Experimental and Computational Studies of Jet Fuel Flow near the Freeze Point

Rajee Assudani,* Jamie S. Ervin,† Steven Zabarnick,‡ and Linda Shafer§
University of Dayton, Dayton, Ohio 45469-0210

To study the flow behavior of jet fuel at low temperatures, a wing-tank thermal simulator, which represents the fuel tank of a commercial aircraft, was fabricated. The simulator was subjected to cooling in an environmental chamber. Experimental results show that fuel flowability and pumpability decrease substantially as temperature is reduced. Time-dependent temperature and velocity distributions were numerically simulated for static cooling. Viscosities were obtained from viscometer measurements using different jet fuel samples. It was observed that near the freeze-point temperature, low freeze-point fuels tend to have higher viscosities than high freeze-point fuels. Measured viscosities were used in computational-fluid-dynamics simulations of jet fuel that was cooled. The calculations show that stringers, ribs, and other structures strongly promote fuel cooling. Also, the cooler, denser fuel resides near the bottom surface of the fuel tank simulator. The presence of an ullage space within the tank was found to strongly influence the fuel temperature profile by sometimes reducing cooling from the upper surface. In other instances, the ullage space enhanced cooling.

Nomenclature

g	=	gravity constant, m/s^2
h	=	enthalpy, J/kg
k	=	thermal conductivity, W/m · K
p	=	pressure, Pa
S^Φ	=	source term
t	=	time, s
u	=	velocity component in x direction, m/s
v	=	velocity component in y direction, m/s
w	=	velocity component in z direction, m/s
x, y, z	=	coordinate directions
Γ_Φ	=	transport coefficient
μ	=	dynamic viscosity, kg/m · s
υ	=	kinematic viscosity, m^2/s
ρ	=	density, kg/m^3
Φ	=	assigned variable in Eq. (1)

I. Introduction

COOLING of jet fuel that takes place during aircraft operation at high altitudes for long flight periods can result in reduced fuel fluidity with the potential for fuel crystallization and gelation. At these low temperatures, fuel viscosity must remain sufficiently low to not impede adequate flow through narrow passageways in fuel lines, filters, screens, and valves. In addition, the viscosity must remain sufficiently low to permit proper boost and engine pump operation and provide appropriate fuel atomization and facile ignition in the engine combustor. Thus, it is essential to study how fuel system operation with fuel temperatures in the vicinity of the freeze point will affect fuel viscosity, which, in turn, influence flow and heat transfer. [The freeze point (ASTM D2386) is actually a melting point and is determined by measurement of the temperature at which the last visible crystal melts upon heating of solidified fuel.] The recent opening of new long-duration polar routes results in fuel tanks being subjected to lower temperatures for longer periods.

Long-duration commercial flights are currently limited to operation under conditions where the measured fuel temperature is 3°C above the fuel specification freeze point. The specification freeze points are −40°C for Jet A fuel and −47°C for Jet A-1 fuel (ASTM D1655). As a consequence, aircraft are restricted to operations where fuel temperatures remain above −37°C for Jet A fuel and −44°C for Jet A-1 fuel. When the measured in-tank fuel temperature approaches these low temperature limits, pilots are forced to modify flight path, altitude, and/or airspeed to raise these temperatures. However, many fuel samples exhibit measured freeze points that are significantly lower than the specification freeze point. Figure 1 shows the frequency of occurrence of fuel freeze points for a random sampling of Jet A fuels measured at North American airports. (Davidson, F., "Phase Technology," private communication 2001). The figure shows that fuels most commonly exhibit freeze points from 2 to 5°C below the specification requirement, but a significant fraction have lower freeze points, with the lowest freezing fuels exhibiting freeze points nearly 18°C below the specification. Thus, for a significant fraction of fuels use of the measured freeze point would permit aircraft operation at lower fuel temperatures during flight, resulting in more flexibility in flight profiles. Increased flexibility in flight altitude and route can result in significant advantages for airlines and their customers, including lower costs and greater flight availability. However, it is important to assess the safe operability of the fuel system at these lower fuel temperatures.

Commercial aircraft fuel tanks usually contain temperature sensors that provide the crew with limited information on the fuel temperature within a subset of the aircraft fuel tanks. Such a single sensor within a fuel tank can provide incomplete and misleading temperature information. Thus, it is important to understand better the temperature distribution within aircraft wing tanks so that temperature sensors can be properly located and the temperature that

Received 4 March 2005; accepted for publication 16 October 2005.

*Graduate Student, Department of Mechanical and Aerospace Engineering, 300 College Park.

†Professor, Department of Mechanical and Aerospace Engineering and Group Leader, Modeling and Simulation, University of Dayton Research Institute, 300 College Park; jamie.ervin@notes.udayton.edu. Associate Fellow AIAA.

‡Group Leader, Fuel Science, University of Dayton Research Institute and Professor, Department of Mechanical and Aerospace Engineering, 300 College Park.

§Research Chemist, University of Dayton Research Institute, 300 College Park.

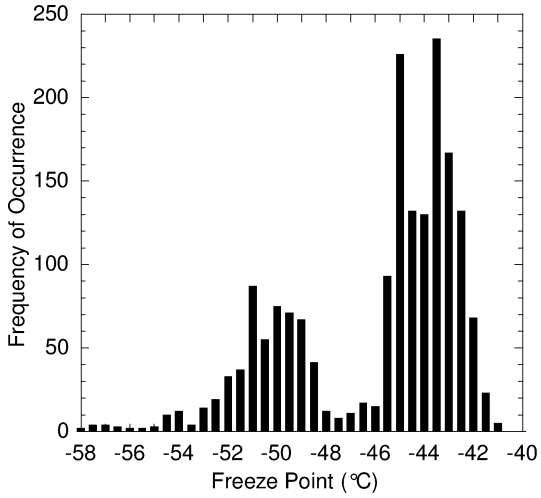

Fig. 1 Frequency of occurrence of fuel freeze points for a sampling of Jet A fuels measured at North American airports (from Davidson, F., "Phase Technology," private communication, 2001).

corresponds to a given sensor can be estimated. Also, in wide-body aircraft such as the Boeing B747, fuel in the outboard main tanks is subjected to the lowest temperatures because these tanks cannot be used until near the end of a long flight. Fuel in these tanks is subjected to the lowest temperatures for long periods. Therefore, it is important to simulate the cooling of a buoyancy-driven flow in these wing tanks.

In the present work we have designed and fabricated a wing-tank simulator that can be subjected to a variety of temperatures inside an environmental chamber to study the effect of low temperatures on jet fuel properties and fuel system operation. The simulator, representing the fuel system components of a commercial aircraft, was run under conditions similar to those found in the aircraft outer wing tank during long-duration flights. The simulator employs actual Boeing B747 fuel hardware, such as flapper valves and a fuel boost pump. Thermocouples in the wing simulator provide temperature measurements within the tank at discrete locations. Computational-fluid-dynamics (CFD) techniques provide the transient thermal behavior of the entire tank. CFD techniques permit the three-dimensional numerical simulation of the complex flow and heat-transfer environment within the tank and assist the understanding of laboratory experiments.

Previous experimental and computational studies of fuel tanks at low temperatures have been performed by Boeing and Lockheed.[1,2] These studies concentrated on temperatures significantly below the fuel freeze point, where fuel solidification begins to occur. This previous work focused on the implications of fuel solidification on fuel hold-up in aircrafts tanks. In these studies, the transient boundary temperatures for the top and bottom surfaces were controlled via heat exchangers. The temperatures of the vertical surfaces were not controlled, but were well insulated. It was assumed that the largest changes in temperature would occur in the direction normal to the top and bottom surfaces, and that the vertical surfaces of the tanks were adiabatic. Although this assumption aids the interpretation of the experiments, it is not completely valid because of the imperfections of the actual insulation. Thus, numerical simulation of these experiments is difficult as the true boundary conditions of the vertical walls are unknown. For the present simulator, transient temperatures are measured on all boundary surfaces. Previous thermal simulations of wing tanks have been limited to simple, circular, or rectangular, two-dimensional tank geometries.[3,4] The wall temperatures were assumed constant, and temperature-dependent jet fuel properties were not used. In the present calculations, we use complex tank geometries, transient boundary temperatures, and measured temperature-dependent fuel properties to more accurately simulate the flow and heat transfer in these complicated systems.

In the current work, we have concentrated our measurements and simulations on the temperature regime near the measured freeze point of the fuel, where the fuel, for the most part, remains a single liquid phase. The simulator is subjected to chilling under controlled conditions and is used to verify three-dimensional predictions of the transient fuel temperature distribution and fuel motion. In the experiments performed, the emphasis was on nearly static cooling. Thus, in all simulations the flow is not pumped, but rather, is driven by buoyancy forces resulting from the transient cooling of the fuel tank. In addition, temperature-dependent fuel properties are used. The viscosity of jet fuel is not readily available for temperatures below -40°C. Here, the viscosity is obtained from low temperature scanning Brookfield dynamic viscosity measurements, as it can vary significantly at temperatures near the freeze point. (The term "viscosity" in this paper represents the dynamic viscosity unless otherwise specified.) The objective of this work is to understand better the effects of temperature on the fuel flowability and pumpability near the freeze point, as well as to elucidate the primary heat transfer and buoyancy-driven flow effects in fuel tanks at low temperatures. During static cooling of the tank, the fuel temperatures are measured. In addition, the fuel temperatures are measured while the fuel is recirculated using a boost pump. CFD techniques are used to calculate the time-dependent temperature distribution in the fuel tank and to analyze the effects of low-temperature properties on the fuel flow. The computations are used to advance the understanding of the influence of the ullage space on the heat transfer in the tank and the resulting fuel temperature profile.

II. Experimental

Commonly used aircraft for long-duration flights include the various varieties of the Boeing B747 (see Ref. 5). Therefore, all of the experimental and most of the simulation work reported here are directed towards the tank design of this aircraft. To understand better the effect of low temperature on aircraft fuel systems, a wing tank simulator, which uses actual B747 components, was fabricated. Figure 2 shows the simulator, which is made of aluminum (internal dimensions $77.5 \times 50.8 \times 50.8$ cm) and includes a baffle rib in the center with three "flapper" check valves (4.7 cm diam). In addition, there are two aluminum Z-stringers (7.6 cm high) positioned at the bottom of the tank that run the length of the simulator. These Z-stringers are supporting structures in an actual fuel tank and have elliptical 1.25-in. (3.18-cm) "limber" holes to allow fuel flow between the stringer divided sections. A single boost pump (Hydro-Aire, Model 60-98976-2), used for each engine in the Boeing 747-400, is powered by a Hobart/AXA 2200, 400 Hz, 115/200V, 7.5-kVA frequency converter/power supply. Also a 16-mesh screen has been installed in the boost pump inlet. This screen is significantly finer, which results in a more conservative flow test than the four-mesh screen used in the inlet of the B747 aircraft. The top of the tank is closed with a plexiglass plate. The simulator is designed so that the fuel can be gravity drained, pumped out via the boost pump, or recirculated through the boost pump back to the tank through a "piccolo" return tube. The entire tank is contained within an environmental chamber (Tenney Environmental, Model T64C15SPL), which can provide a minimum temperature of -73°C. The chamber is

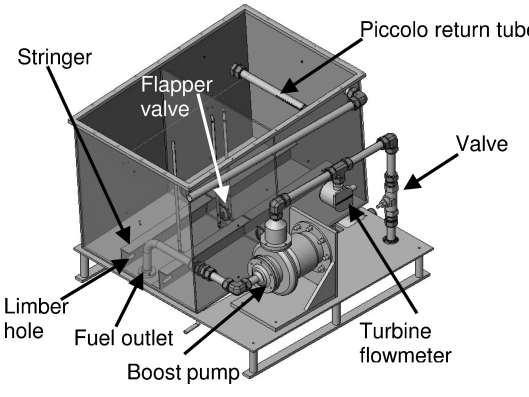

Fig. 2 Drawing of the wing-tank simulator.

sufficient to produce a low-temperature environment similar to that expected for aircraft flying at high altitudes for long periods. For safety concerns, the environmental chamber is purged with nitrogen, and nitrogen resides in the fuel-tank ullage space. The pressure within the fuel tank is maintained at normal atmospheric pressure.

The wing-tank simulator was instrumented with a series of 48 thermocouples, a flowmeter, and pressure gauges. Vertical temperature profiles were obtained at three locations in the tank. A post was located near the center of each of the two internal chambers (created by the single baffle rib) for the mounting of thermocouples. A third post was installed near a side wall to obtain boundary temperatures. Thermocouples were also mounted internally on the side walls and the inside bottom surface of the tank. A thermocouple was located on the boost pump housing to measure the pump temperature. Thermocouples were also located in the pump inlet and outlet to measure the fuel temperature rise caused by pump operation. A calibrated turbine flowmeter was located downstream of the pump. Pump power measurements could be obtained from current and voltage measurements of the three-phase power supplied to the pump. Thermocouple, flow, and pressure measurements were obtained at 10-min intervals during cooldown from ambient conditions and at 1-s intervals during pump operation.

Two types of tests using the wing-tank simulator are reported here: static cooldown and recirculation. In static cooldown tests, the fuel was cooled from ambient temperature down to a given target temperature near the fuel freeze point while monitoring fuel and tank temperatures without flow. In recirculation tests, the fuel was cooled down (typically overnight) to a target temperature (usually a temperature slightly below the measured freeze point of the fuel). When the target temperature was reached, the pump was started and the fuel recirculated back to the tank through the piccolo tube. The fuel temperature would slowly increase because of heat input from the pump. Recirculation continued until the fuel temperature reached the high-temperature target, usually -37°C. The fuel recirculation typically lasted one to two hours.

Viscosity is one of the most important fuel properties to consider when studying the effect of temperature on fuel flowability and pumpability. Viscosity measurements were performed using a scanning Brookfield Viscometer (Tannas, Plus two). As the fuel sample (30 mL) is cooled from -40 to -65°C at 5°C/h, the viscosity is measured continuously by the increasing torque generated by a spindle rotating in the fluid at constant speed (12 rpm). The viscosity measurements are anchored at -40°C by calibrating to measurements obtained at the same temperature using ASTM D445, which measures the time for a volume of liquid to flow under gravity through a calibrated glass capillary viscometer.[6] Freeze-point data were acquired using a Phase Technology PSA-70V Petroleum Analyzer via ASTM D5773.

III. Simulation Methodology

A commercially available CFD code (CFD-ACE, ESI Group) was used to simulate the laminar, time-varying flow and heat transfer by finite volume solution of the unsteady, three-dimensional Navier–Stokes and energy (enthalpy) equations.[7] Equation (1) represents the momentum or energy equation depending on the variable represented by Φ (velocity component or enthalpy, respectively).

$$\frac{\partial(\rho\Phi)}{\partial t} + \mathrm{div}(\rho \boldsymbol{u}\Phi) = \mathrm{div}(\Gamma_{\Phi}\,\mathrm{grad}\,\Phi) + S^{\Phi} \qquad (1)$$

For a given Φ, Γ_{Φ} is the appropriate transport coefficient, and S^{Φ} is the source term. With respect to the momentum equation, buoyancy forces induced by temperature differences within the tank are included in S_{Φ}. In addition, the viscous dissipation was neglected. Table 1 lists the transport coefficients Γ^{Φ} and the source terms S^{Φ} of the governing equations.

The convective terms are represented by a third-order-accurate upwind scheme, and a version of the SIMPLEC (semi-implicit method for pressure-linked equations consistent) algorithm is used in the solution procedure.[7] To study the effect of an ullage space on heat transfer and flow within the tank, the interface between the liquid fuel and air can be tracked by techniques, such as the volume-of-fluid (VOF) method.[8,9] Unfortunately, the VOF method requires excessive computation time for the long time periods considered in the present simulations. For simplicity, only the behavior of the bulk liquid fuel is simulated, and flow and thermal boundary conditions at the liquid–air interface are imposed. The calculations were simplified by assuming an adiabatic fuel–air interface. This assumption is reasonable because the convective heat-transfer coefficient on the air side of the interface is small ($\sim$1 W/m^2 $^{\circ}$C) for natural convection. In addition, because the bulk behavior of the media was the focus, surface tension was neglected. Hence, the fuel–air interface was assumed to be planar. The viscosity of the air is orders of magnitude smaller than that of the fuel. Thus, it was assumed that the shear stresses on the fuel at the interface were negligible.

Table 1 Source terms and transport coefficients appearing in Eq. (1)

Φ	Γ^{Φ}	S^{Φ}
u	μ	$-\frac{\partial p}{\partial x} + \frac{\partial}{\partial x}\left(\mu\frac{\partial u}{\partial x}\right) + \frac{\partial}{\partial y}\left(\mu\frac{\partial v}{\partial x}\right) + \frac{\partial}{\partial z}\left(\mu\frac{\partial w}{\partial x}\right)$
v	μ	$-\frac{\partial p}{\partial y} + \frac{\partial}{\partial x}\left(\mu\frac{\partial u}{\partial y}\right) + \frac{\partial}{\partial y}\left(\mu\frac{\partial v}{\partial y}\right) + \frac{\partial}{\partial z}\left(\mu\frac{\partial w}{\partial y}\right) + \rho g$
w	μ	$-\frac{\partial p}{\partial z} + \frac{\partial}{\partial x}\left(\mu\frac{\partial u}{\partial z}\right) + \frac{\partial}{\partial y}\left(\mu\frac{\partial v}{\partial z}\right) + \frac{\partial}{\partial z}\left(\mu\frac{\partial w}{\partial z}\right)$
h	k	0

Table 2 Measured freeze point, total weight percent normal alkanes, and viscosities of jet fuels studied

Fuel sample ID	Fuel type	Freeze point, $^{\circ}$C	Viscosity (cP) at freeze point	Total weight percent normal alkanes
3688	Jet A	-41.6	10	20.7
3686	Jet A	-41.9	8	14.6
2827	Jet A	-42.9	10	20.6
3166	Jet A	-43.7	15	21.6
3219	Jet A	-46.4	19	18.3
4336	JP-8	-47.2	19	15.2
3804	JP-8	-47.6	15	23.6
4339	JP-8	-48.6	13	23.4
3658	Jet A	-53.1	25	7.1
3633	Jet A	-55.1	18	19.1
4177	JP-8	-57.2	25	12.3
2976	JPTS	-58.5	17.5	17.2

A three-dimensional unstructured grid representing the fuel tank simulator was employed. The three-dimensional geometry of the simulator involves two compartments, separated by a baffle plate that has three circular passages available for flow. In the simulations, the actual "flapper" valves are represented by holes for simplicity, as the actual valves offer little flow resistance. Also, two Z-stringers, 7.6 cm high located at the bottom of the tank, are included in the calculations. Because only the static flow was simulated, the piccolo tube was not included in the calculations. For the ullage case, structured grids were used instead of unstructured grids as the structured grids required less computation time.

When the global error residuals were reduced below four orders of magnitude from their maximum values, the solution was considered to be converged. A coarse grid was first made with fewer cells and was further refined by increasing the number of grid points until grid independence was achieved. Three-dimensional structured grids representing the fuel tank simulator, with different ullage spaces (3.8, 25.6, and 33.8 cm), were studied for grid independence of the solution. Results from a grid with 64,824 cells were found to be grid independent for ullage height of 3.8 cm and are described in this work. Results with 56,010 and 47,736 cells were found to be grid independent for ullage heights of 25.6 and 33.8 cm, respectively. Also, using an unstructured grid for the full tank, calculations obtained from a grid of 159,862 cells were grid independent. Further grid refinement resulted in negligible changes in the solutions.

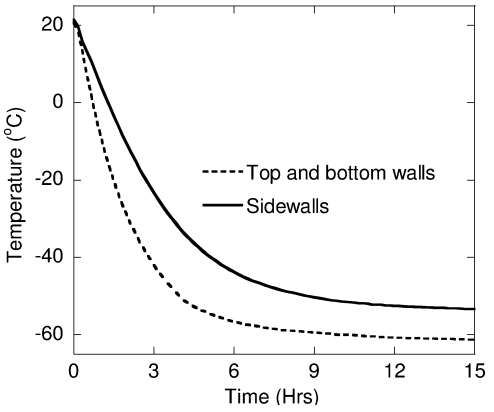

Fig. 3 Wall-temperature schedule used for the cooling simulations.

For the current simulations, the temperature-dependent viscosity of fuel sample 3166 (Jet A) is used as this fuel was used in the experiments. Viscometer measurements (already described) provided the temperature-dependent fuel viscosity for the simulations. Table 2 shows properties of 12 jet fuels that were selected for their relatively wide range of freeze points. In addition, the temperature-dependent values of the density, thermal conductivity, and specific heat of Jet A fuel compiled by the Coordinating Research Council were used in all simulations.[10] As they vary slowly and linearly in region below −40°C, values of density, thermal conductivity, and specific heat were linearly extrapolated from higher temperatures.

The temperature boundary conditions for the simulations come from a spatial average of the thermocouples embedded in the walls. These spatial averages are represented as a function of time and used as the transient temperature boundary condition in the calculations. The initial air and fuel temperature is assumed to be uniform. Figure 3 shows the temperature boundary conditions employed in the static cooldown simulations. With the set point of the environmental chamber fixed, the chamber was allowed to reach a low temperature of its own accord. The fuel is initially at 20°C, and the top and bottom walls decrease uniformly in time from 21 to −61.2°C, while the side walls decrease to −53.3°C, after 15 hours.

IV. Results and Discussion

Here, the effect of ullage on heat transfer and fuel temperature is described using computational and experimental data. In addition, simulations of heat transfer and flow during static cooling are validated with the experimental measurements. The effects of low temperature and viscosity on heat transfer, pumpability, and flowability are presented. (Jet A is the fuel used in all numerical simulations.)

A. Effect of Ullage Space on Tank Heat Transfer

To better understand the implication of the location of fuel-tank temperature sensors and the distribution of fuel temperatures within fuel tanks during cooling, experimental measurements and CFD simulations of fuel cooling in the wing-tank simulator were performed. These studies simulate the fuel cooling that occurs in aircraft wing-tanks upon exposure to the low-temperature environment at altitude. The subsequent section describes the heat transfer and flow for conditions in which the tank is entirely filled with fuel. However, aircraft fuel tanks are almost never entirely full and thus usually have ullage spaces above the fuel. Even when a flight starts with a completely full tank, fuel use during the flight results in ullage formation during the flight. Thus, the effect of varying levels of ullage space on the resulting heat transfer and fuel temperature distribution are studied. Ullage heights of 3.8, 25.6, and 33.8 cm were studied. The volume of these three ullage spaces is 15,000, 100,000 and 130,000 cm^3, respectively. These simulations follow the wall temperature schedule of Fig. 3.

Figures 4a–4c show that the calculations agree reasonably well (within 3°C) with the temperature measurements for different ullage spaces at three different thermocouple locations. Simulations with an air gap of 3.8 cm were performed for 2.5 hours, whereas all the other simulations were performed for four hours. The calculations show that the model can be used successfully to predict the temperature profiles in an aircraft fuel tank. Figure 5a shows a calculated temperature contour plot representing 2.5 hours of cooling for the full tank relative to Figs. 5b and 5c, which represent the calculations with an air gap. Much of the fuel near the center of the tank remains at a relatively warm temperature. Figure 5b shows that when a small ullage space is present (3.8 cm in height) the fuel temperature is significantly higher (about 5°C) than the full tank case.

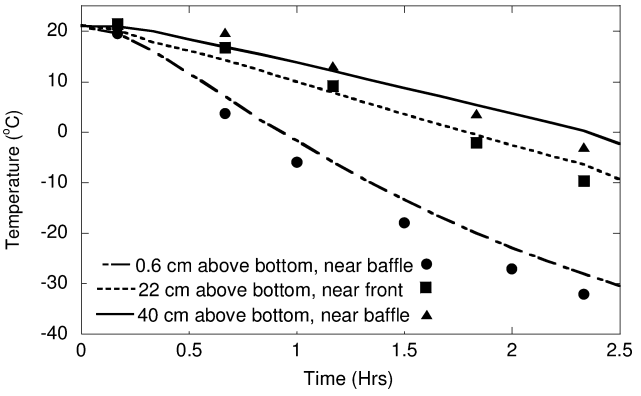

Fig. 4a Measured and simulated temperatures for Jet A fuel in the tank with an ullage space (3.8-cm height) for three different thermocouple locations. The symbols represent measured temperatures.

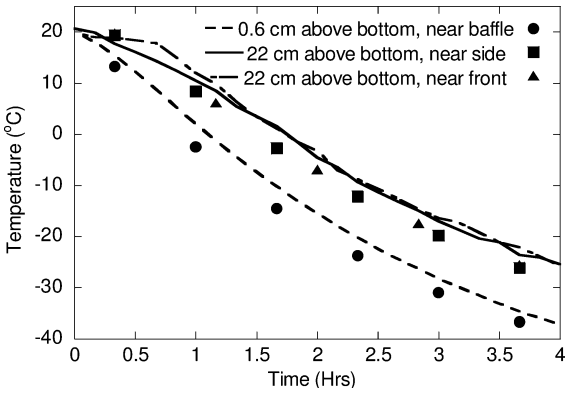

Fig. 4b Measured and simulated temperatures for Jet A fuel in the tank with an ullage space (25.6-cm height) for the three different thermocouple locations. The symbols represent measured temperatures.

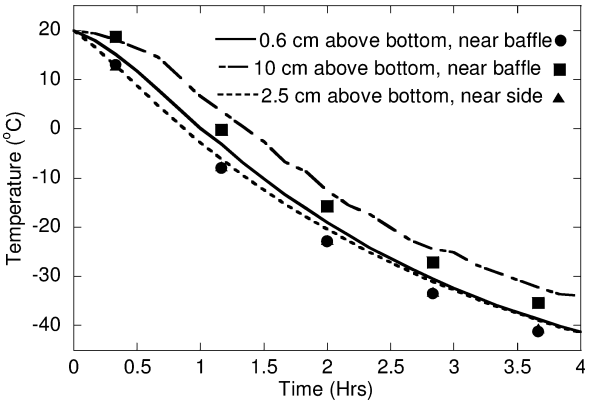

Fig. 4c Measured and simulated temperatures for Jet A fuel in the tank with an ullage space (33.8-cm height) for the three different thermocouple locations. The symbols represent measured temperatures.

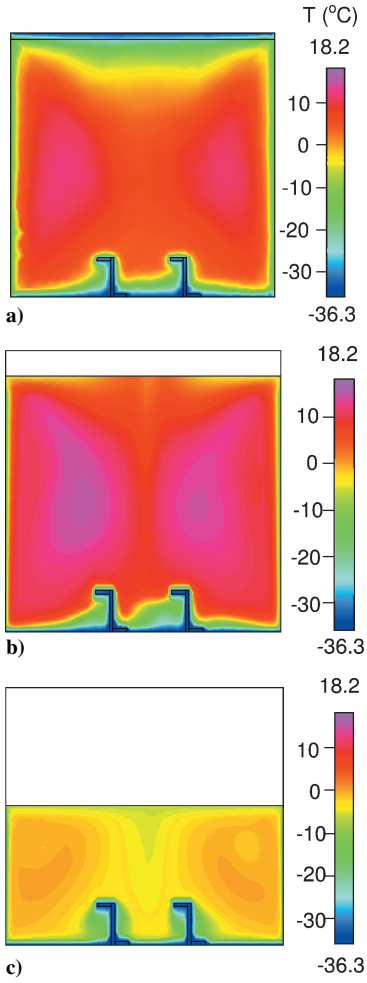

Fig. 5 Temperature contours of Jet A fuel for three-dimensional simulations after 2.5 hours of cooling near the center of a tank compartment for a) full tank and inclusion of air gap heights of b) 3.8 cm and c) 26.5 cm.

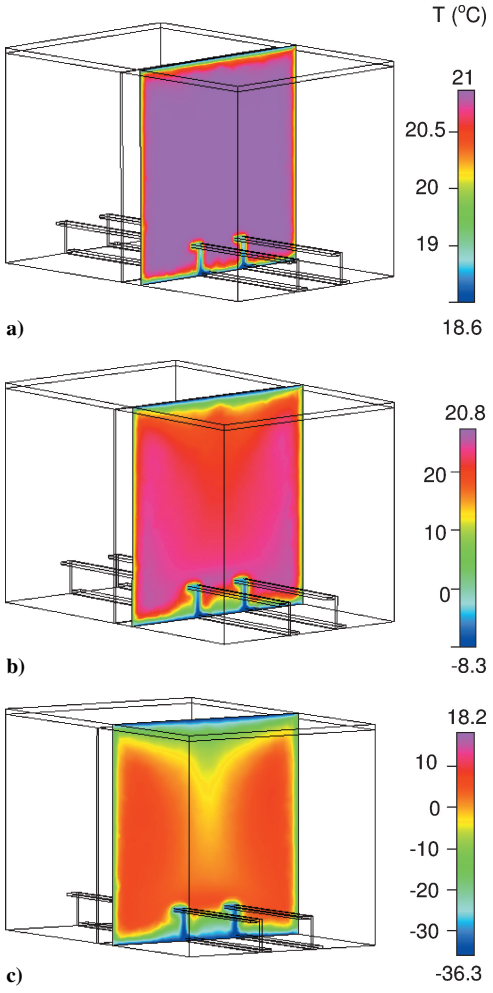

Fig. 6 Three-dimensional temperature color contour plots of the Jet A fuel within the tank after a) 10 min, b) 1 h, and c) 2.5 hs.

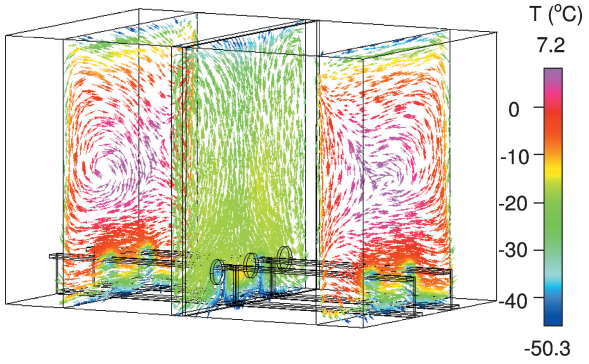

Fig. 7 Vector plot showing three different locations in the tank simulator from a three-dimensional calculation for Jet A fuel after four hours.

This difference demonstrates that the heat transfer from the top surface has a significant effect on the fuel temperature. Thus in the full tank case, this increased heat transfer from fuel contact results in lower fuel temperatures. In contrast, in the small ullage space case, the presence of air limits the heat transfer with the top surface and results in higher fuel temperatures. Interestingly, when the ullage height is increased to 25.6 cm (Fig. 5c), the fuel temperatures are even lower than in the full tank case. These lower temperatures are a result of the significantly lower fuel volume and increased surface-area-to-volume ratio, which results in faster cooling. These results show that a relatively small ullage space results in increased fuel stratification and higher fuel temperatures relative to a full tank or a large ullage space. Aircraft fuel tanks are rarely completely filled with fuel, but the varying dihedral wing angle during flight results in portions of the tank having a wetted top surface, whereas other portions will have varying amounts of ullage space. In addition, the relative amount of these two regions will vary as fuel is consumed during flight. Thus, the implications of the presence or absence of ullage space in fuel tanks on heat transfer and fuel temperature are extremely complex and dependent on numerous flight conditions.

B. Heat Transfer and Flow During Static Cooling in a Full Tank

Figures 6a–6c show the results of three-dimensional temperature calculations (via two-dimensional viewing planes near the center of the tank) at times up to 2.5 hours of cooling. Figure 6a shows that after 10 min a thermal boundary layer develops, and fuel temperatures near the baffle plate reduce to nearly 7°C. As the cooling proceeds, stratification in the tank increases. Figures 6b and 6c show an increase in the thermal boundary layer after one and 2.5 hours, respectively. Flow of cold fuel flowing from the top surface can be observed. Most of the fuel near the baffle plate reduces to nearly −3 and −23°C after two and four hours of cooling, respectively. Figure 7 shows the velocity vector plot demonstrating the development of a complex flow pattern in the three-dimensional calculation at four hours. The velocity vectors shown are proportional to the velocity magnitude, which vary over the range 0 to 0.048 cm/s. The vector plots show that the flow pattern is similar but opposite in direction for the two fuel compartments. Also, for a location near the baffle rib, the flow is more complex, and the temperature there is much lower than elsewhere in the tank because of the increased heat transfer caused by the baffle rib. Also, the thermal boundary

layer around the stringers, causes increased convective motion and stratification. The results demonstrate that much of the heat conduction occurs through the stringers, and the colder, more dense fuel tends to be located near the bottom of the tank. Because more dense fuel tends to be located near the tank bottom, it is much preferred to locate the thermal sensors near the tank bottom.

C. Low-Temperature Flowability and Pumpability Measurements

Experiments using the wing-tank simulator were conducted to assess the effect of low temperatures on fuel flowability and pumpability. These tests examined a series of fuels (JP-8, Jet A, Jet A fuel with a low temperature flow improving additive, and JPTS–fuel properties shown in Table 2) in which cooldown and recirculation runs were performed. JPTS (freeze-point specification −53°C) and JP-8 (freeze-point specification −47°C) fuels are refined to provide improved low-temperature capability beyond Jet A fuels. They were chosen to provide a comparison of the flowability of these improved low-temperature fuels with that of Jet A. During the recirculation tests, fuel was cooled down to a target temperature near the freeze point and subsequently pumped via the boost pump out the fuel inlet and back into the tank via the piccolo return tube. The pump operation results in heat being added to the fuel. This added heat resulted in a slow fuel temperature rise (approximately 20°C per hour) during recirculation. Fuel recirculation was continued until the fuel reached the target temperature of −37°C, which is 3°C above the Jet A specification maximum freeze point and an operational limit for commercial flights. In this way, this fuel recirculation method is used to evaluate the fuel flowability and pumpability over a range of temperatures in a single experimental run.

Figure 8 shows that, for each fuel, as the temperature increases the flow rate increases. This observation results primarily from the decrease in viscosity with increasing temperature shown later in viscometer measurements. The flow rates at 3°C above the measured freeze-point temperature (shown as vertical arrows for each fuel in the figure) can be compared with the flow rates at −37°C for each fuel. Over this temperature range, flow reductions of 2.2, 4.1, 9.2, and 10.2% are observed for fuels 3166, 3804, 4177, and 2976, respectively. These data show that the low freeze-point fuels exhibit greater flow reduction relative to the −37°C temperature than do high freeze-point fuels. This important result shows that operating fuels near their measured freeze point rather than near the specification freeze point can result in reduced fuel flowability, in agreement with the viscometry measurements. The important question is how such a reduction in fuel flowability will affect aircraft and engine operation. The answer to this question is likely fuel-system dependent. Each aircraft fuel system would need to be evaluated individually to evaluate the flow-rate requirements of the engine. In addition, it is also important to take into account the effect of the engine main pump on fuel flow. For example in the B747 aircraft, suction from engine main pump operation can lessen the observed effect.

Figure 8 also shows a comparison of the flowability of a fuel containing a candidate cold flow-improving additive (referred to here as additive 4314) with that of the unadditized fuel. The figure shows that the additized fuel remained flowable to temperatures almost 15 deg below the fuel freeze point. In the temperature range where the two fuels overlap, their flow rates remained nearly identical. It is hypothesized that the additives modify crystal morphology to attain improved low-temperature fluidity.[6,11] At very low temperatures and long residence times, crystals continue to nucleate and grow and ultimately increase the effective viscosity of the liquid–solid mixture, regardless of crystal morphology. Nevertheless, the current results indicate that flow-improving additives hold promise for providing jet fuels with improved reduced temperature capabilities.

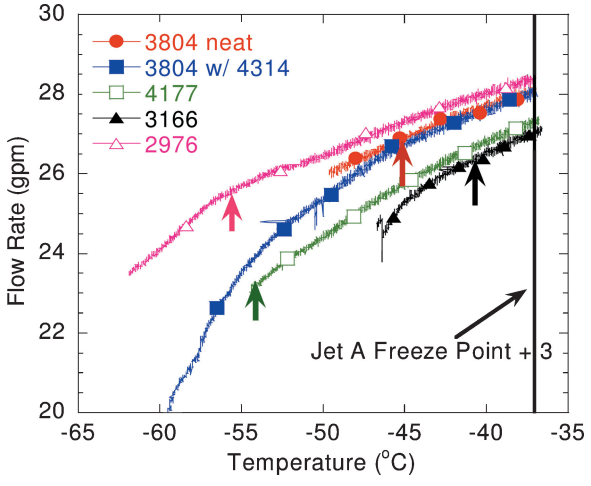

Fig. 8 Plots of flow rate vs temperature during recirculation in the wing-tank simulator using five different fuels. The vertical arrows represent the measured freeze point plus 3°C for each fuel. The vertical black line shows the Jet A specification plus 3°C (−37°C).

D. Role of Viscosity in Heat Transfer and Flowability

Viscosity is one of the most important fuel properties to consider when studying the effect of temperature on fuel flowability and pumpability. Viscosity is a measure of the resistance to flow of a fluid. The specification for Jet A and Jet A-1 fuels, ASTM D1655, as well as the specification for JP-8 fuel, MIL-DTL-83133E, require a maximum kinematic viscosity of 8.0 cSt measured at −20°C. Because the temperature of the fuel is much higher at the engine than in the fuel tanks, specifications for fuel viscosity are not given below −40°C. The viscosity specification was designed to ensure adequate fuel flow through fuel lines, valves, and pumps at reduced temperature. In addition, the viscosity specification also ensures proper fuel atomization in engine combustors. The performance of combustor nozzle atomizers, as well as subsequent proper fuel evaporation and mixing with air, are strongly dependent on the fuel viscosity. Engine manufacturers usually specify a maximum fuel kinematic viscosity of 12 cSt at the nozzle to ensure reliable engine starting performance. The standard viscometry technique used for specification measures kinematic viscosity by measuring the time required for a fixed volume of fuel to flow through a calibrated capillary tube. This test is performed at the desired fixed temperature. In the present studies, we have chosen to measure the dynamic viscosity via a Scanning Brookfield Viscometer. This technique offers the advantage of being able to rapidly measure viscosity as a function of temperature. Such measurements would be extremely time consuming and/or impractical using the capillary tube technique.

Figure 9 shows plots of dynamic viscosity vs temperature using the scanning Brookfield technique for nine fuel samples. This technique measures dynamic viscosity rather than kinematic viscosity as in the ASTM D445 method. The dynamic viscosity μ can be related to the kinematic viscosity υ via the density ρ by $\mu = \upsilon\rho$. The figure shows that the fuels display a very slow rise in viscosity as they are cooled below −40°C. Upon further cooling, the fuels display a relatively sudden, rapid increase in viscosity. Previous work has

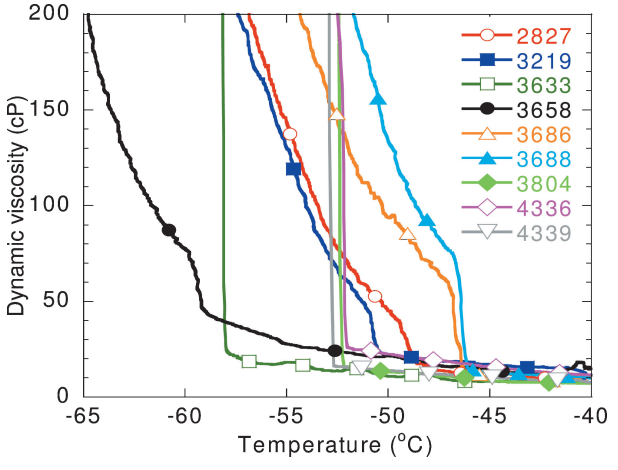

Fig. 9 Measured viscosities of nine jet fuel samples.

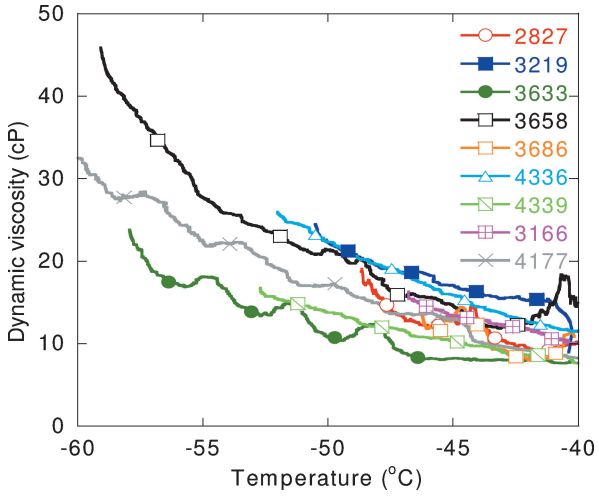

Fig. 10 Measured liquid-phase viscosities of nine jet fuel samples.

shown that this sudden, rapid rise in viscosity occurs very close to the measured cloud point (ASTM D5773-95) and that microscopic crystal formation begins at this temperature.[6] These observations support the conclusion that this increase in viscosity is caused by the occurrence of solid crystal formation in the fuel, as the cloud point is the temperature at which visible solids are first observed upon cooling. For the current study, we are most interested in how the liquid-phase viscosity varies with temperature. To show this variation better, we have deleted the portions of the viscosity in the crystallization regime (i.e., the high-viscosity regime), rescaled, and replotted this liquid-phase only data in Fig. 10 for the nine jet fuel samples.

Figure 10 shows how the liquid-only dynamic viscosity changes with temperature over a range of jet fuel samples. The figure shows that, in general, there is a gradual rise in viscosity over this temperature range. More interestingly, it is apparent that fuels with relatively high cloud/freeze points have relatively low viscosities at their cloud/freeze point, whereas fuels with low cloud/freeze points have relatively high viscosities at their cloud/freeze point. (The cloud point is near the lowest viscosity measurement for each fuel.) These results have important implications for fuel system operation. The results show that there may be issues in using the fuel freeze point (which is usually 2 to 6°C above the cloud point) to evaluate fuel flowability. For example, the low-temperature freezing fuel 3658, which has a freeze point of −53.1°C and a cloud point of −59.2°C, displays a viscosity of 46.4 cP at its cloud point, whereas fuel 3688, which has a freeze point of −41.6°C and a cloud point of −46.1°C, has a viscosity of 11.7 cP at its cloud point. This factor of four difference in viscosity can have a significant effect on fuel flowability and pumpability at these temperatures. Despite these differences near their cloud point temperatures, these two fuels display very similar viscosities in the temperature range −40 to −45°C. The significance of this factor of four difference in viscosity will depend on the specific fuel system requirements, such as required flow rate for the engines, ability of the fuel system pumps to handle higher viscosity fuel, and the efficiency of combustor nozzle to atomize higher viscosity fuel. This observation of increased viscosity near the freeze point of lower freeze-point fuels relative to high freeze-point fuels is an important issue to consider when deciding whether to use low freeze-point fuels at temperatures below the specification freeze point. These data show that it is important to consider the effect that this increase in viscosity will have on fuel flow to the engine and on fuel atomization in the combustor. Studies in the wing-tank simulator just reported further elucidate how low temperatures affect viscosity and the resulting fuel flowability and pumpability in actual fuel system components.

It is interesting to consider why lower freeze-point fuels have higher viscosities near their freeze point than do high freeze-point fuels. One possible explanation relates to the ideality of the jet fuel mixture in the liquid phase vs the solid phase. It is known, in the temperature region in which crystallization begins, that the incipient solid crystals consist of highly nonideal solid solutions of the larger normal alkanes (such as C_{16}–C_{19}) present in the fuel.[12] These large normal alkanes make up only a small fraction of the total normal alkane concentration. In contrast, the remaining liquid fuel displays mixture properties that are very close to ideal. Thus, the crystallization of normal alkanes from the fuel, and therefore the freeze point, is highly dependent on the concentration and identity of these species. The liquid mixture should display ideal mixture viscosity behavior, with the resulting viscosity being a function of the bulk of the species present. Numerous components within jet fuel contribute to the overall viscosity of the fuel mixture, and the contribution of each species also depends upon its concentration within the fuel.[13] The freeze point is more dependent on the distribution of the largest normal alkane species.[13] Thus the viscosity is a function of the overall distribution of contributing species within the fuel, although the freeze point is more dependent on the distribution of the largest normal alkane species. Therefore, if two fuels differ only in the concentration of the larger normal alkanes, the one with the higher level of large normal alkanes will exhibit a higher temperature freeze point (Table 2). Because the distribution of the remaining species remains the same, these fuels should have similar viscosities. However, the lower freeze-point fuel will crystallize at lower temperatures, where the liquid viscosity will be higher than that of the higher freeze-point fuel at its freeze point. Thus, the observation that lower freeze-point fuels display higher viscosities near their freeze points likely results from the fact that the viscosity is mostly a function of the bulk species present, while freeze point is more sensitive to the concentration of the larger normal alkanes present.

Figure 10 shows that fuel samples that meet a particular fuel specification can have very different viscosities at the same temperature. Thus, it is important to understand how changes in viscosity can influence the flow and temperature within a cooled fuel tank. We have employed our simulation methodology with a three-dimensional grid for the present calculations. The dynamic viscosity used in the calculation was increased by either 30% ($1.3\mu_0$) or 200% ($3\mu_0$) above that of the measured baseline fuel (μ_0) as shown in Fig. 11. These relatively large changes in viscosity are studied because large changes in viscosity do occur upon cooling jet fuels, as shown in Fig. 10. Figure 12 shows the calculated temperature contours obtained after four hours of cooling using each of the three viscosity vs temperature curves from Fig. 11. The temperature contours represent a two-dimensional viewing plane near the center of a tank compartment. The figures indicate that there is increased mixing and fluid motion when the fuel viscosity is low. The figures also show that less convective motion and an increase in temperature throughout the tank can be observed when the viscosity is increased. The result is an increase in fuel stratification with increasing viscosity. The calculation predicts the temperature at the center of a tank compartment to be −13.7°C for μ_0, −11.2°C for $1.3\mu_0$, and −4°C

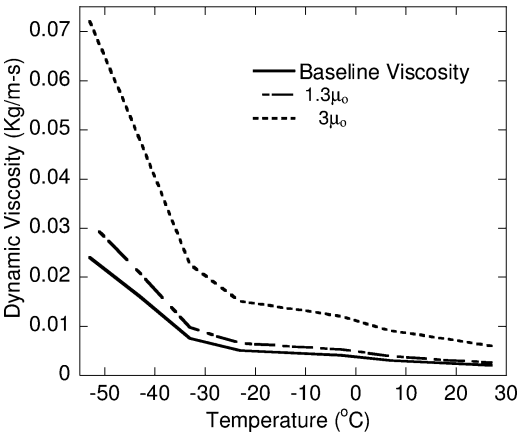

Fig. 11 Plot for increase in dynamic viscosity by either 30% ($1.3\mu_0$) or 200% ($3\mu_0$) relative to the baseline density (μ_0).

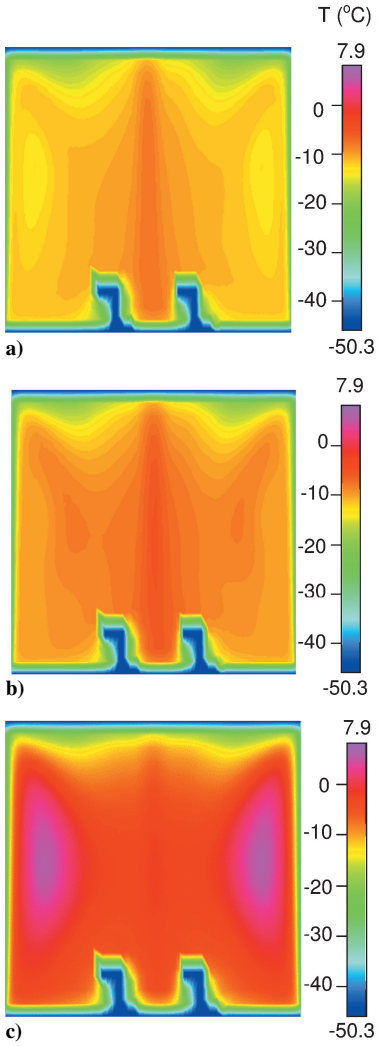

Fig. 12 Three-dimensional time-varying simulations of the fuel temperature after four hours of cooling for a) viscosity = μ_0, b) viscosity = 1.3μ_0, and c) viscosity = 3μ_0.

for 3μ_0, after four hours. Thus, a 30% viscosity increase has little effect on the bulk fuel temperature, whereas a 200% increase can alter fuel temperatures by 10°C. These calculations show that it is important to know the range of typical fuel viscosities as a function of temperature that are encountered during aircraft operation and use these typical viscosity ranges when locating tank temperature sensors and evaluating fuel tank designs.

V. Conclusions

In the present work, the flowability and pumpability of jet fuel were studied to determine how changes in fuel properties at low-temperature affect jet aircraft fuel system operation. Both experiments and computations were employed to elucidate aspects that affect fuel temperature. Measurements and simulations of cooling of a static tank show complex flow and heat-transfer effects. Heat transfer in the tank was found to be significantly increased by the presence of baffle ribs, stringers, and other structural members. The presence of the Z-stringers greatly increases heat transfer and stratification near the tank bottom. The results show that fuel-tank temperature sensors need to be located near the tank bottom to reasonably measure low fuel-tank temperatures. In addition, the location and geometry of structural members should be considered in the thermal design of a fuel tank.

Calculations were also performed on the effect of ullage level on fuel temperatures and heat transfer. The results show that a relatively small ullage increased fuel temperature stratification, with higher temperatures in the tank center relative to a completely filled tank. A large ullage space can lead to reduced temperatures because of the relatively small fuel volume and high surface-to-volume ratio.

Evaluation of the effect of temperature on fuel flowability and pumpability was conducted in a wing-tank simulator. The results show that flowability and pumpability decrease substantially as temperature is reduced. The measurements show that low freeze-point fuels exhibit greater flow reduction than do high freeze-point fuels. This indicates that operating fuels near their measured freeze point rather than near the specification freeze point can result in reduced fuel flowability. This needs to be evaluated based on the requirements of individual aircraft fuel systems.

In support of the simulator measurements, viscosity measurements as a function of temperature show that lower freeze-point fuels tend to have higher viscosities near their freeze point than do higher freeze-point fuels. These lower viscosities result in the lower flow rates observed in the wing-tank simulator. The higher viscosity of low freeze-point fuels at their freeze point likely results from the fact that the freeze point is a strong function of the larger normal alkanes present, while viscosity reflects the overall normal alkane fuel composition. Large variations (greater than 100%) in the viscosity of different fuel samples were found to be necessary to produce significant effects on the heat transfer within the fuel tank.

Acknowledgments

This work was sponsored by the Federal Aviation Administration, Airport and Aircraft Safety Research and Development Division, AAR-400, located at the William J. Hughes Technical Center, Atlantic City International Airport, New Jersey (Skip Byrnes, technical monitor) under Contract DTFA03-01-C-00038. Also, this material is based on research sponsored by Air Force Research Laboratory under agreement number F33615-03-2-2347.

References

[1]Mehta, H. K., and Armstrong, R. S., "Detailed Studies of Aviation Fuel Flowability," Boeing Commercial Aircraft Co., NASA CR-174938, Jan. 1985.

[2]Stockemer, F. J., "Experimental Study of Low Temperature Behavior of Aviation Turbine Fuels in a Wing Tank Model," NASA CR-159615, Aug. 1979.

[3]McConnell, P. M., Owens, S. F., and Kamin, R. A., "Prediction of Fuel Freezing in Airplane Fuel Tanks of Arbitrary Geometry—Part 1," *Aircraft Engineering*, Vol. 58, No. 9, 1986, pp. 2–7.

[4]McConnell, P. M., Owens, S. F., and Kamin, R. A., "Prediction of Fuel Freezing in Airplane Fuel Tanks of Arbitrary Geometry—Part 2," *Aircraft Engineering*, Vol. 58, No. 9, 1986, pp. 20–23.

[5]Zabarnick, S., Laber, M., Ervin, J., and Assudani, R., "Operation of Aircraft Fuel Systems at Low Temperatures," *Proceedings of the 8th International Conference on Stability and Handling of Liquid Fuels*, International Association for Stability, Handling, and Use of Liquid Fuels, Atlanta, Sept. 2003, pp. 162–191.

[6]Zabarnick, S., and Vangness, M., "Properties of Jet Fuels at Low Temperature and the Effect of Additives," *Preprint-American Chemical Society*, Div. Pet. Chem., Vol. 47, Washington, DC, 2002, pp. 243–246.

[7]"CFD-ACE (U) Users Manual," CFD Research Corp., Huntsville, AA, Jan. 2002.

[8]Hirt, C. W., and Nichols, B. D., "Volume of Fluid (VOF) Method for the Dynamics of Free Boundaries," *Journal of Computational Physics*, Vol. 39, No. 1, 1981, pp. 201–225.

[9]Rider, W. J., Kothe, D. B., Mosso, S. J., Cerrutti, J. H., and Hochstein, J. I., "Accurate Solution Algorithms for Incompressible Multiphase Fluid Flow," AIAA Paper 95-0699, Jan. 1995.

[10]*Handbook of Aviation Fuel Properties*, Coordinating Research Council, Atlanta, 1983.

[11]Ervin, J. S., Zabarnick, S., Binns, E., Dieterle, G., Davis, D., and Obringer, C., "Investigation of the Use of JP-8+100 with Cold Flow Enhancer Additives as a Low-Cost Replacement for JPTS," *Energy Fuels*, Vol. 13, No. 6, 1999, pp. 1246–1251.

[12]Coutinho, J. A. P., "A Thermodynamic Model for Predicting Wax Formation in Jet and Diesel Fuels," *Energy Fuels*, Vol. 14, No. 3, 2000, pp. 625–631.

[13]Atkins, D. L., Ervin, J. S., and Shafer, L., "Experimental Studies of Jet Fuel Viscosity at Low Temperatures, Using a Rotational Viscometer and an Optical Cell," *Energy Fuels*, Vol. 19, No. 5, 2005, pp. 1935–1947.